

Scanning the Crack

ATLAS LArG CBT-EC2 Report

J.Rutherford
12 July 2004

The goal of the ATLAS LArG 2nd EndCap Combined Beam Test (CBT-EC2) in summer 2004 is to scan the two overlapping transitions between the EMEC/HEC and the FCal. However it was discovered that the modules are too low in the H1 cryostat to adequately cover the entire transition (crack) region. This report describes the problem, discusses the various constraints, and proposes a solution.

Hermetic calorimetry is a strong feature of the ATLAS detector. One aspect is the almost seamless transitions between calorimeter subsystems. However small these transitions might be, ATLAS will still do its best to correct for their effects on the data. Investigation of the transitions between the EMEC/HEC and the FCal was a part of the standard Liquid Argon test beam program as outlined in the ATLAS Liquid Argon Calorimeter Technical Design Report, page 521 [1]. But due to the limited size of the H1 cryostat it was recognized that special HEC modules would have to be built and this required substantial resources beyond the already stretched construction funding. The possibility to cover the goals of this test in a full test of the EndCap Cryostat in the X5 beam line and discouraging responses to attempts to secure funding for the special modules led to a decision at the ATLAS LArG EndCap Workshop at Ringberg to cancel this test. But when plans for the X5 beam test were abandoned and the LHCC expressed its enthusiasm for this study, attempts to secure funding for the special modules were redoubled and eventually succeeded.

Specifically, the goals of the CBT-EC2 are to determine 1) the corrections to both the energy (see Fig. 1) and angle when energy flows into this crack region between the calorimeters and is absorbed in the structural and dead material and/or leaks out, 2) the rms fluctuations in this loss of energy and offset flow direction, and 3) the tails on the energy and angle distributions as input to the calculation of the instrumental backgrounds to the signal for large E_T^{miss} (see Fig. 2). This last measurement drives the statistical precision required from the test beam data.

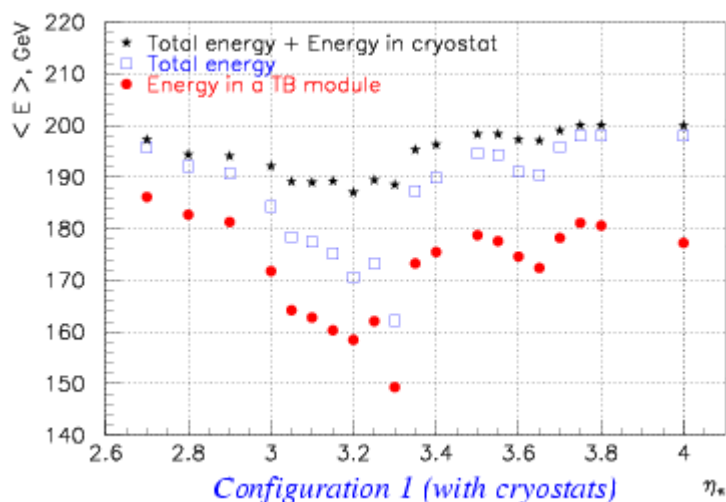


Figure 1: Average energy deposited in various volumes by 200 GeV charged pions as seen with GEANT3 simulations [2]. The effect of the transitions shows as a loss of energy deposited in the Test Beam modules starting at $\eta = 2.9$ and ending near $\eta = 3.7$.

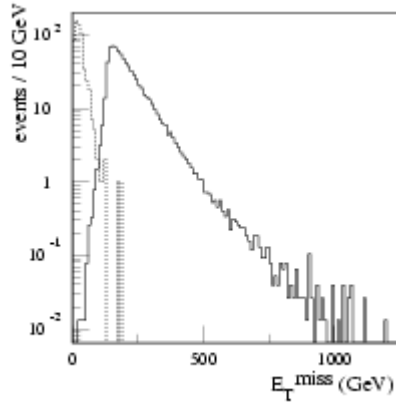


Figure 2. The solid line shows the reconstructed ΣE_T for the jet(s) in $Z + \text{jet(s)}$ events where $Z \rightarrow \mu\mu$ and a cut on $p_T(Z) > 200$ GeV is applied. The dashed line is the “measured” E_T^{miss} for such events, including known instrumental effects, when no E_T^{miss} is expected [3].

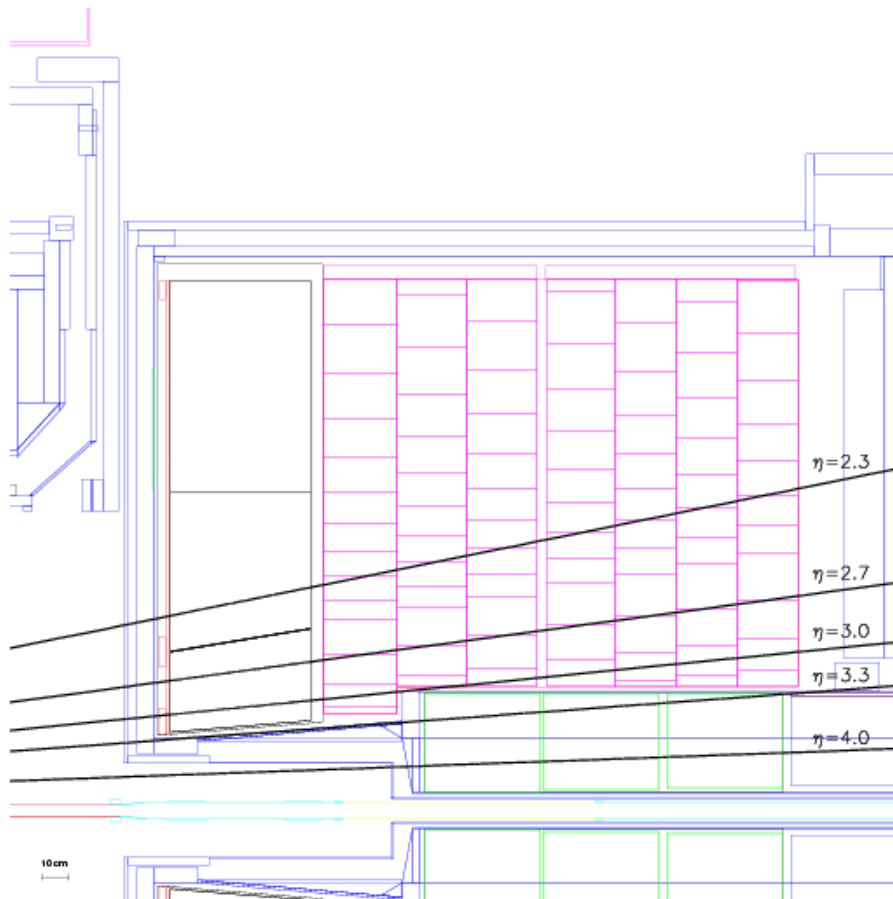


Figure 3: GEANT3 geometry description of the calorimeter modules in the EndCap Cryostat with lines of constant η superimposed [2]. Note that the transition between the HEC and FCal falls between $\eta = 3.0$ and $\eta = 3.3$. The transition between the EMEC and FCal is projective between $\eta = 3.2$ and $\eta = 3.3$. The line $\eta = 2.8$ (not shown) is roughly in the center of the EMEC inner wheel module.

All the way back to the Liquid Argon Calorimeter TDR [1] it was planned to center the acceptance of the modules near $\eta = 2.8$. We failed to check the consequences of this choice, in detail.

Figure 3 shows a few lines of fixed η superimposed on a GEANT3 description of the modules in the EndCap Cryostat. The transition between the HEC and FCal includes 1) the cryostat support tube, an aluminum tube 8 mm thick which holds the FCal modules, 2) about 12 mm of liquid argon, and 3) structural material at the HEC inner radius to hold the HEC modules together. In the test beam, an 8 mm aluminum section of a cylinder simulates this structural member. This transition starts at about $\eta = 3.0$ and continues to at least $\eta = 3.3$. The transition between the EMEC and FCal includes 1) some structural material at the $\eta = 3.2$ edge of the EMEC, 2) some liquid argon, and 3) the forward cone at $\eta = 3.3$. This 8 mm thick aluminum cone is another structural member of the cryostat and is simulated in the test beam with a cone section of the same dimensions. The distance between the smallest angle particles to still hit the EMEC and the largest angle particles to just miss the cone at the z-coordinate of the cone is more than 30 mm. Both the simulated cone and simulated cylinder are fastened to a simulated washer or bulkhead in front of FCal1. This “washer” is another structural member of the EndCap Cryostat.

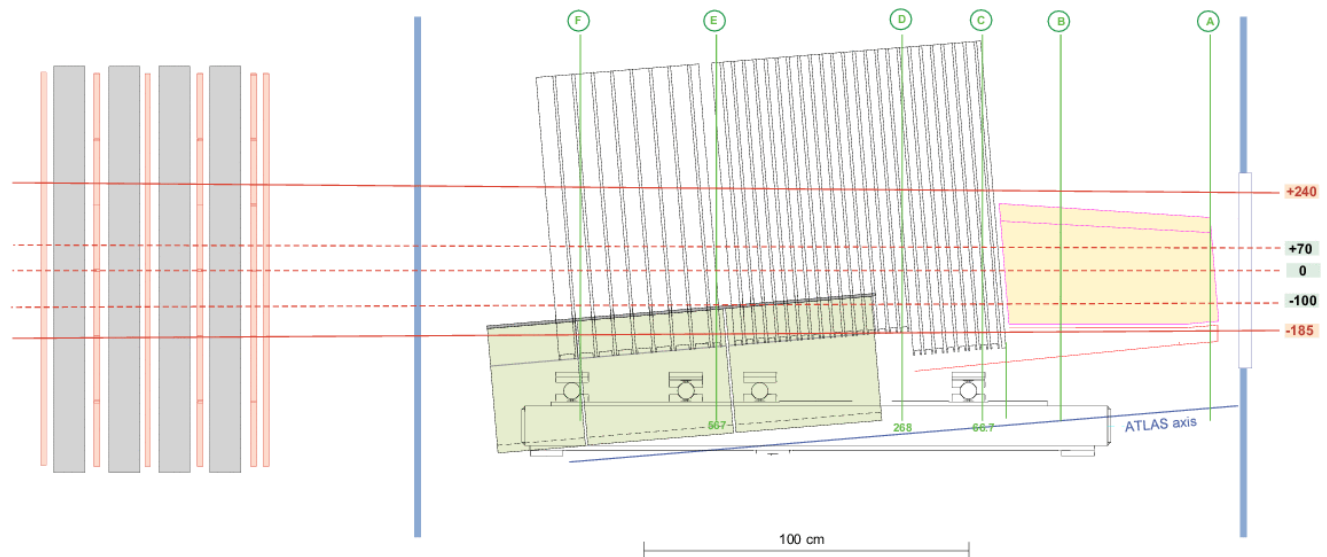


Figure 4. Elevation drawing (provided by L.Kurchaninov) of the EMEC, HEC, and FCal modules in the H1 cryostat and of the Warm Tail Catcher downstream of the cryostat. The H6 test beam comes in from the right. The beam is steered vertically by the beam line magnet designated Bend 9. Beam particle trajectories emanating from the effective bending center of Bend 9 are superimposed.

Early in the CBT-EC2 run, close inspection of the drawings suggested we would have trouble scanning the full crack region with beams of momentum of 200 GeV/c, the highest momentum available in the H6 beam line. In the crack region near $\eta = 3.2$, this momentum corresponds to $E_T \approx 20$ GeV, an already very low value compared to the energies expected from high p_T collisions at the LHC. Drawings prepared to address this question suggested that the present configuration would restrict us to momenta only up to about 120 GeV/c for a full scan of the crack. At higher momenta we could scan into the crack from the EMEC/HEC side but not out of the crack again into the FCal on the other side, that is, we could scan approximately half of the crack region only.

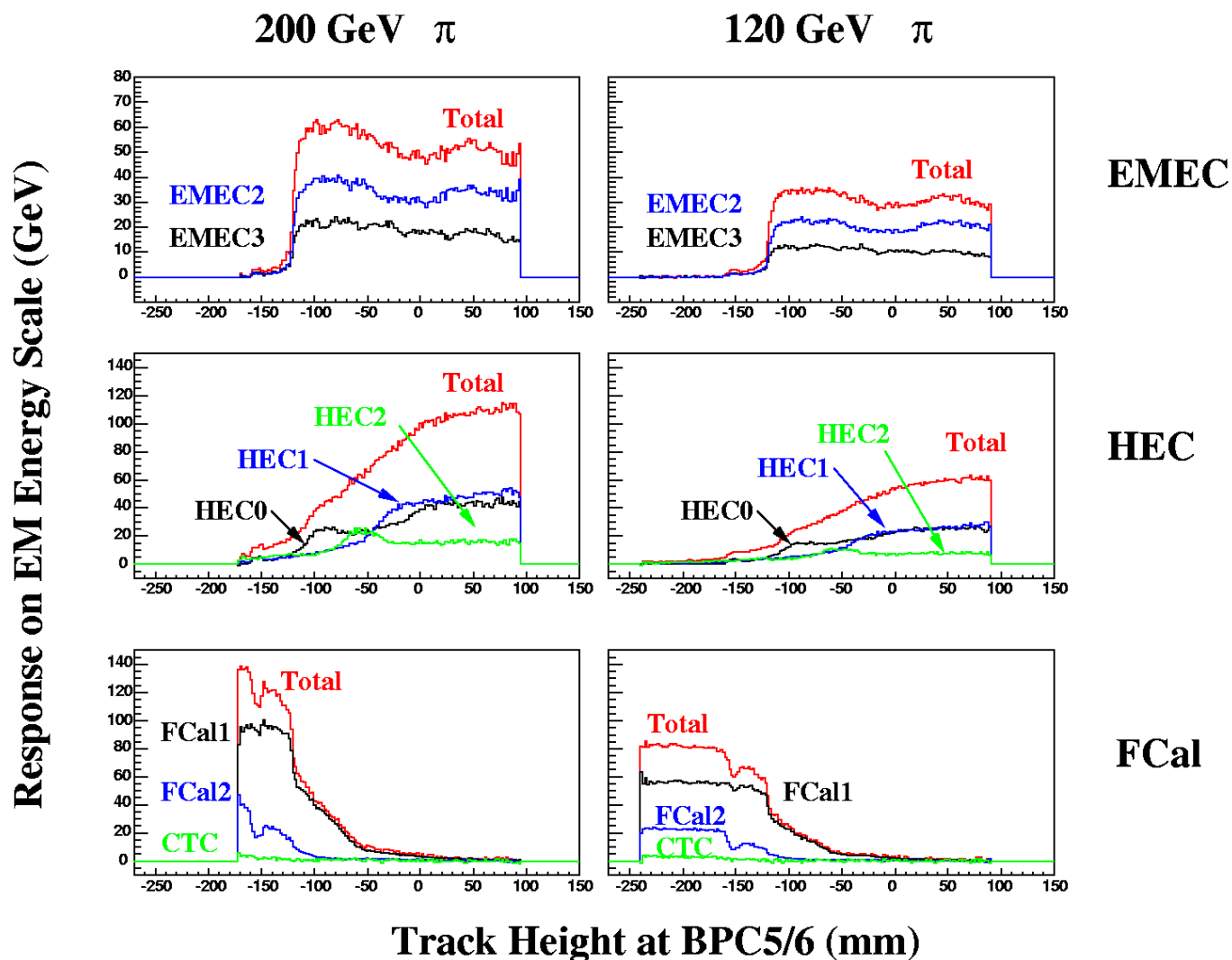


Figure 5. For each calorimeter and for two beam energies, the calorimeter response in a given depth segment is plotted versus the height of the beam track as measured in the last Beam Profile Chamber on the movable table. The “notch” at about -155 mm in the FCal response is probably due to the projective cone, a structural member of the EndCap cryostat and a key element in the transition between the EMEC and FCal. (Courtesy of P.Loch)

The height of the modules in the cryostat was determined via an analysis of early CBT-EC2 data by P.Loch. Fig. 5 shows the energy deposited in each depth segment of the modules as a function of the height of the beam track in the most downstream Beam Profile Chamber (BPC) located near the center of the table. This is the table just upstream of the H1 cryostat on which is mounted trigger and veto counters and wire chambers. It can be moved up and down remotely with precision of order 1 mm. Fig. 6 shows this same data, but this time summed over all the modules, as well as by subsystem. The feature of interest in both figures is the “notch” near -155 mm. This is most likely the cone at $\eta = 3.3$. Note that this notch shows up in both the 120 GeV/c data and the 200 GeV/c data. But we could only see it at 200 GeV/c with “wide” beam, as shown in Fig. 7. The center of the 200 GeV/c beam can only be bent down to -135 mm and therefore cannot reach as low as this important piece of projective dead material.

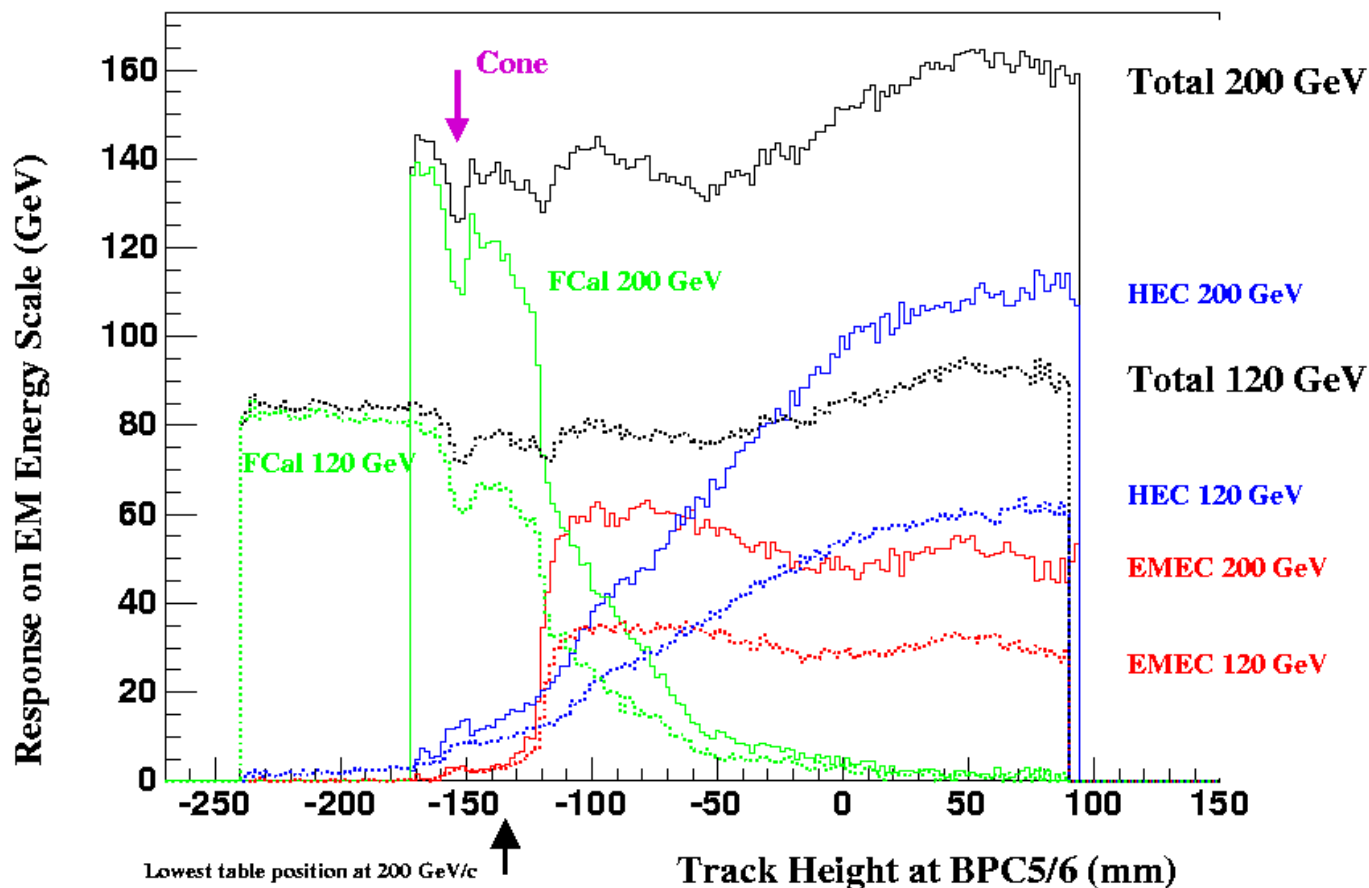


Figure 6. Same as Fig. 5 but summed over depth segments and then summed over modules. The “notch” (the projective cone) clearly shows up at about -155 mm. (Courtesy of P.Loch)

Assuming that the cone is properly identified and its height, as measured by projective beam trajectories at the downstream BPCs, is fixed at -155 mm, then we know the height of all the modules in the cryostat. But this assumes that the simulated cone is properly positioned in the H1 cryostat relative to the modules the same as in ATLAS. Preliminary CBT-EC2 analysis of the position of pad boundaries in the EMEC [4] confirms this assumption with a precision of order 5 mm. I will therefore make this assumption. This data shows the center of the acceptance is not quite at $\eta = 2.8$ as previously supposed but, rather, closer to $\eta = 2.85$. This is shown in Fig. 8. The conclusion is that the test beam modules are a bit higher in the cryostat than we thought.

Survey data shows that the modules in the H1 cryostat are tilted at about 4.8 degrees, corresponding to $\eta = 3.17$. This allows us to pin down the position of the ATLAS interaction point (IP) in the H6 reference frame. The present best estimate is that the IP is located at a point upstream of the midpoint between the last two BPCs by 1200 mm (close to the upstream end of the table) and below the nominal H6 beam by 130 mm.

In order that beam particles at the center of the acceptance appear to originate from the IP we should raise the H1 cryostat by 130 mm. This was the original proposal to enable us to properly scan the crack.

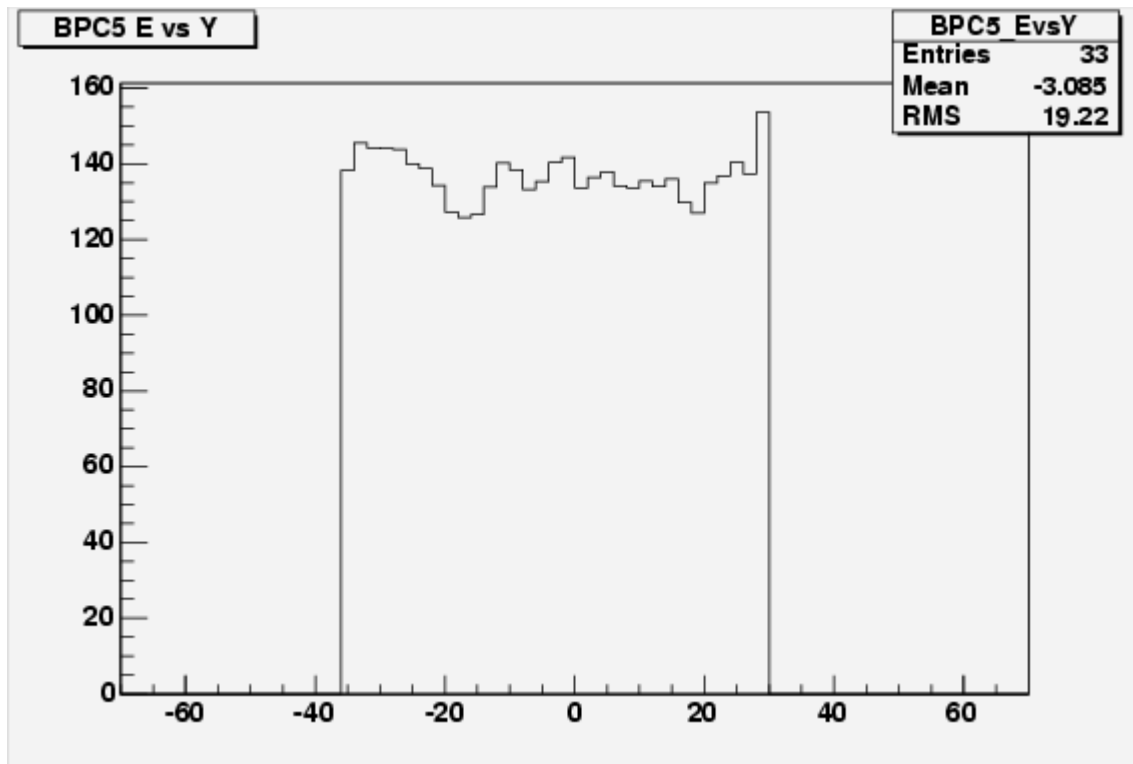


Figure 7. The same as Fig. 5 and 6 but for 200 GeV/c beam and a single run of the composite scan in beam height. Note that the “notch” could only be seen by employing the “wide beam” option because the lowest the 200/c GeV beam can be deflected is at 0 on this plot (the center of the Beam Profile Chamber) which corresponds to -135 mm on the plots in Fig. 5 and 6. Note that the “wide” beam spot is wider here, on the low side, than assumed in this report. (Courtesy of P.Loch)

Raising the cryostat isn't the only option for improving our ability to adequately scan the crack. Because we are limited by the bending power of Bend 9 at 200 GeV/c we have investigated the possibility to increase the bending power by either replacing Bend 9 with a more powerful vertical bending magnet or by adding another vertical bending magnet upstream of the existing Bend 9. There are at least 10 magnets identical to Bend 9 sitting unused in the North Area, so we have recently focused on this second choice. If the present Bend 9 and the additional, identical magnet were wired in series, then the maximum current would remain 1500 A, the maximum voltage would increase by a factor 2, the bending power would increase by a factor 2, and the effective center of bending would move upstream from about 30930 mm to 32650 mm from the midpoint of the two most downstream BPCs.

Moving the effective center of bending upstream and increasing the maximum bending angle presents a problem for the most upstream BPCs. These chambers are fixed in position, i.e. they are not on a movable table. We prefer to leave these chambers as is because they provide the only time-independent reference coordinate system of the test beam run. The wires in the BPC cover a vertical aperture of 120 mm and the BPC window frame is 110 mm high. The region of optimal position resolution is further restricted to about ± 40 mm. At maximum current the new Bend 9 would provide a bending angle for 200 GeV/c beam of about 8.7 mrad. This would move the beam center about 42 mm below the BPC center and the extremes of the “wide” beam would be about 72 mm from the BPC center, i.e. beyond the aperture of the chambers. To compensate we can steer the beam upwards via TRIM5 which is upstream

of Bend 9 by about 41 m. With a maximum B·dℓ about 0.4 Tm at 250 A [5], we can elevate the 200 GeV beam at Bend 9 by about 25 mm.

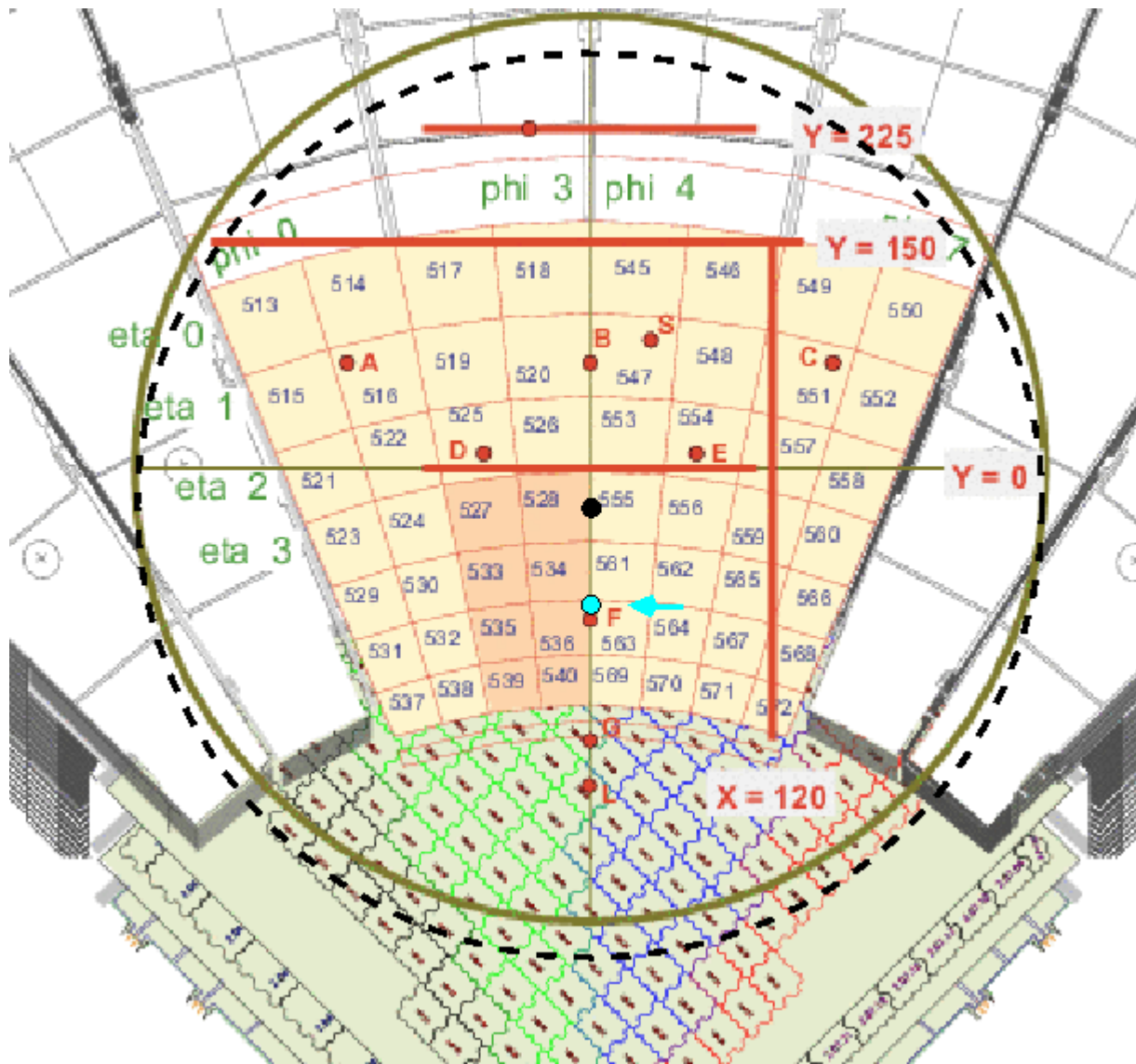


Figure 8. Front view of the modules (courtesy of L.Kurchaninov) showing the presumed center of the acceptance at $\eta = 2.8$. The black dot shows the acceptance center as determined from analysis by P.Loch which found the simulated, projective cone, shown here in outline just below the EMEC (see Fig. 5, 6, and 7). The dashed circle shows the outline of the cryostat window corresponding to the updated acceptance center. The spot indicated by an arrow is where the acceptance center would be if the cryostat is raised by 70 mm. Note that the pad boundaries in the EMEC are projective with respect to the IP and go in steps of $\Delta\eta = 0.1$ starting at $\eta = 2.5$ at the outer radius of the EMEC inner wheel and ending at $\eta = 3.2$ at the inner radius. Points A, B, S, C, D, E, F, G, and L are target points for stability checks.

In this case the extreme beam trajectory for “wide” beam would be about 45 mm from the chamber center which will have to be acceptable.

Another constraint comes from the diameter of the beam pipe and the “wide” beam. Assuming the beam is about 30 mm radius at the position of the Bend 9, the beam pipe is 120 mm in diameter, and the beam center is raised by TRIM5 by 25 mm, the extreme trajectory would be displaced from the nominal beam by 55 mm which is awfully close to the 60 mm allowed by the diameter of the vacuum pipe. We have therefore requested larger beam pipe flanges in the region of Bend 9. The relevant dimensions are shown in Fig. 9.

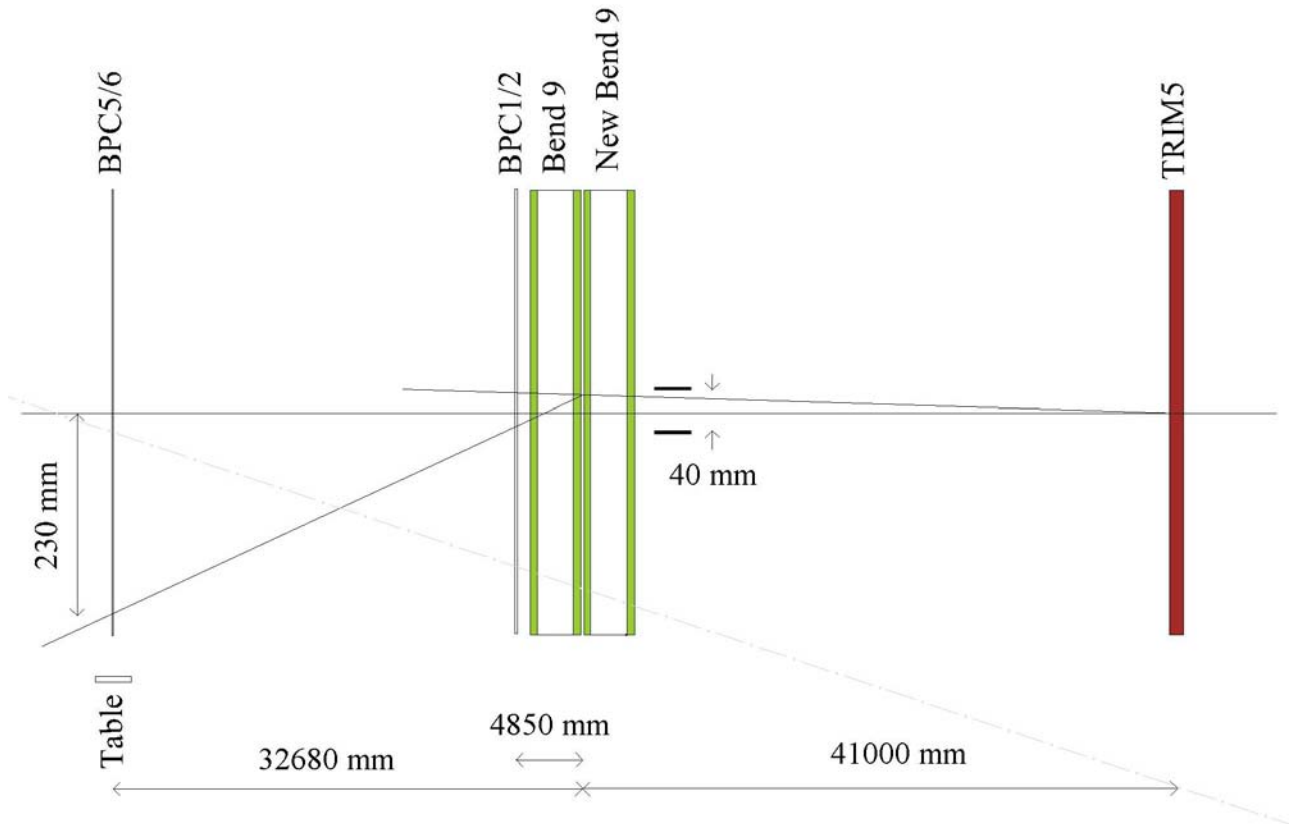


Figure 9. Distorted elevation of the downstream end of the H6 beam line showing TRIM5, the upgraded Bend 9, the upstream BPCs, and the downstream BPCs on the table.

A simple doubling of the bending power of Bend 9 should have allowed us to increase the vertical range of the “narrow” beam from ± 135 mm to over ± 270 mm (the small change in the location of the effective bending point gives a slightly increased range). However the need to keep the beam within the limits of the upstream BPCs via TRIM5 restricts the new range to slightly under ± 230 mm.

The definition of η in the test beam environment is ambiguous. This variable really only makes sense when referred to the ATLAS IP. But because we refer many fiducial points to the ATLAS reference frame I have developed a method to relate values of η to our test beam geometry. The ambiguity is resolved if we specify the transverse plane in which the fiducial point is located. This plane and the value of η (and ϕ) allow a unique definition of any fiducial point. Fig. 4 shows planes A through F which are normal to the H6 beam. These are barely discernable in Fig. 10 which is the same as Fig. 4 but foreshortened along the H6 beam line so the table with the most downstream BPCs can be included. In a root macro I have defined similar planes but normal to the ATLAS beam line rather than the H6 beam

line. As noted earlier these two lines are at about 4.8 degrees to each other so the difference between these two sets of planes is not so great. Otherwise the planes are at about the same z-positions with respect to the modules.

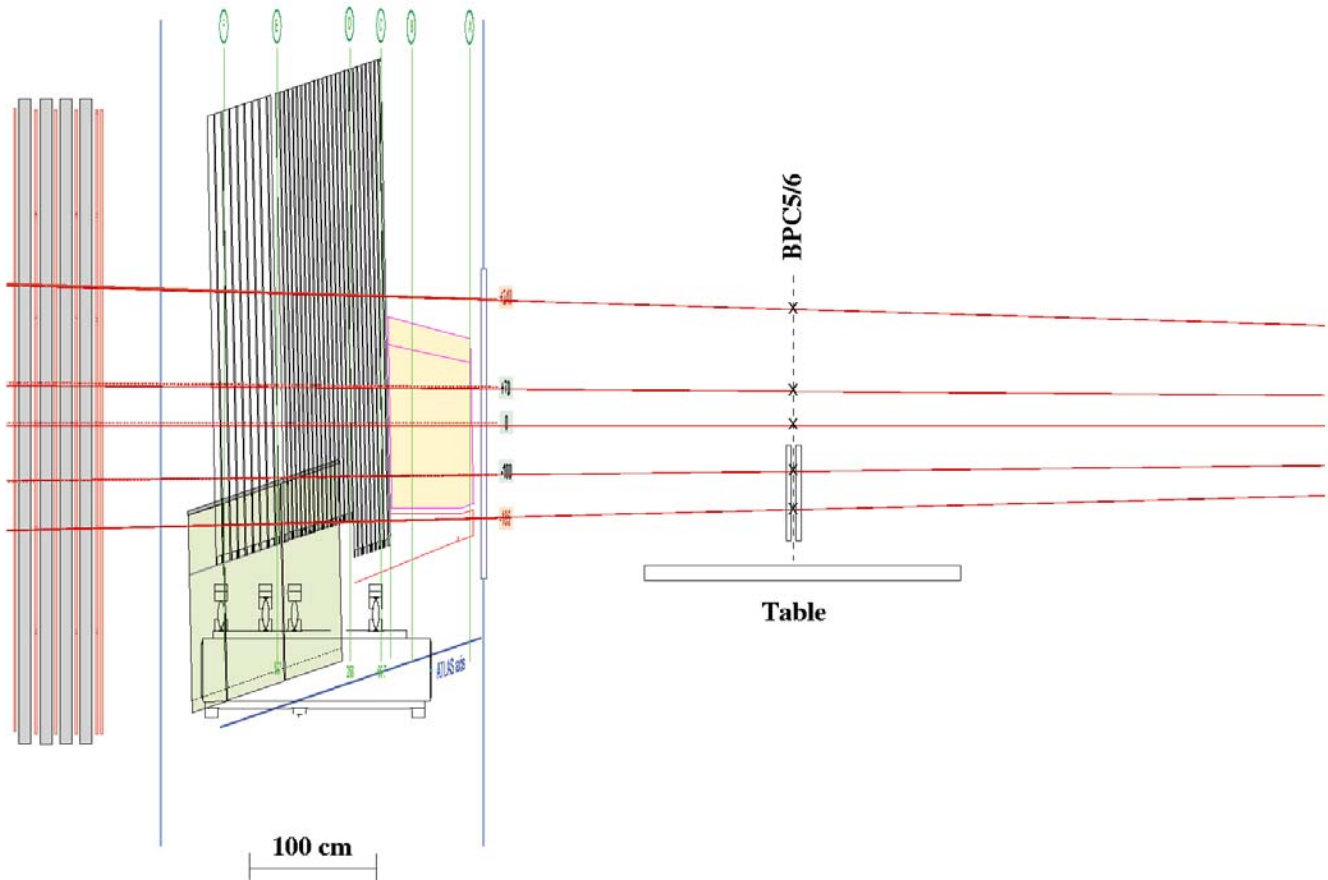


Figure 10. Same as Fig. 4 but distorted so that the table with the Beam Profile Chambers can be seen. Also shown are representative beam particle trajectories emanating from the bend center of Bend 9 further upstream.

Fig. 4 and 10 include test beam particle trajectories emanating from the effective bend point in Bend 9. Any fiducial point in the modules (specified by η , ϕ , and the z-coordinate of the transverse plane, all in the ATLAS coordinate system) can be projected back along such test beam particle trajectories to the vertical (in the H6 coordinate system) “view” plane lying between the two most downstream BPCs on the table. The x-coordinates are not distorted in the same way because the H1 cryostat is moved horizontally to reach off center regions of the modules. This allows a much simpler projection. The root macro makes pictures of such projections which are intended to be an aid in deciding how to optimize the height by which to raise the H1 cryostat.

In the upper right hand corner of each of the following 8 root macro figures a code specifies the view. The first character, an upper case letter, indicates the plane as in Fig. 4 and 10 (but normal to the ATLAS beam rather than the H6 beam). The next character denotes the location of the H1 cryostat. “0” means the cryostat is at its normal height above the floor, “u” means it is raised by 50 mm, “h” means it is raised by 70 mm, and “U” means it is raised by 100 mm.

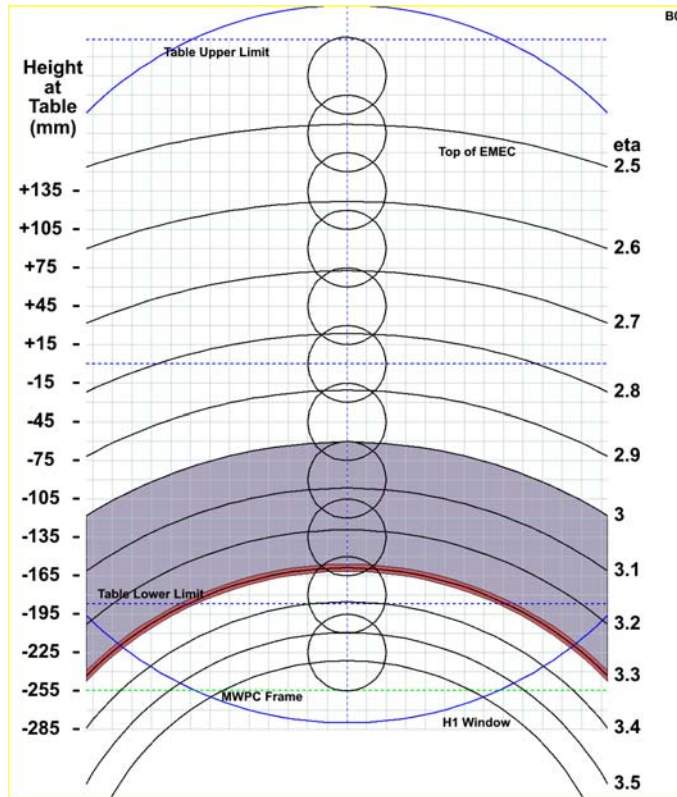


Figure 11. Projected plane at the downstream end of the EMEC with present cryostat position.

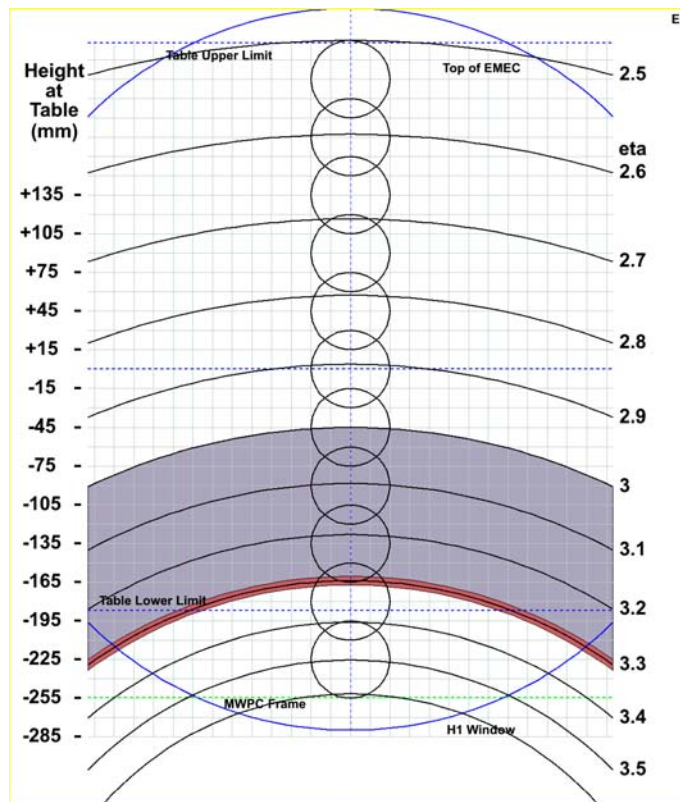


Figure 12. Projected plane at the front face of FCal2 with present cryostat position.

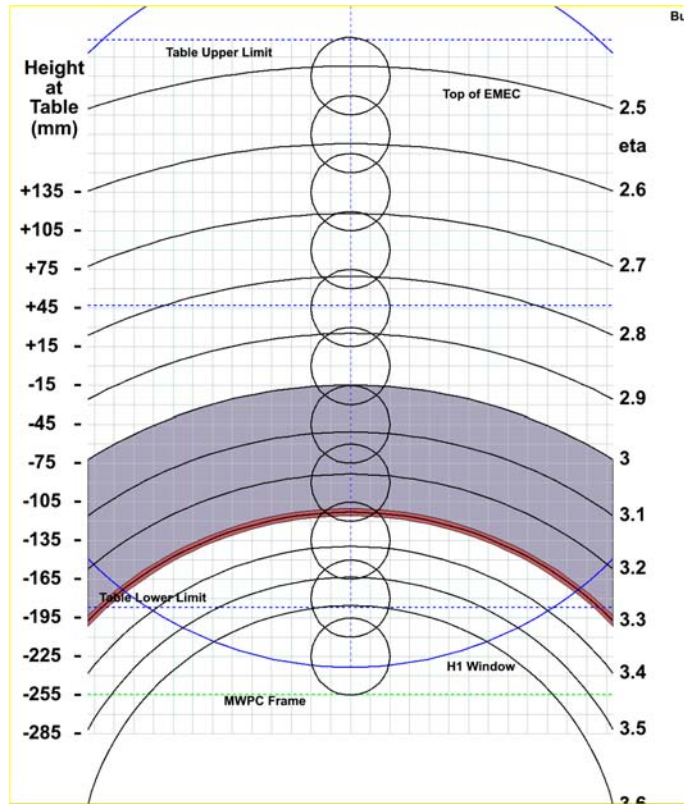


Figure 13. Projected plane at the downstream end of the EMEC with cryostat raised by 50 mm.

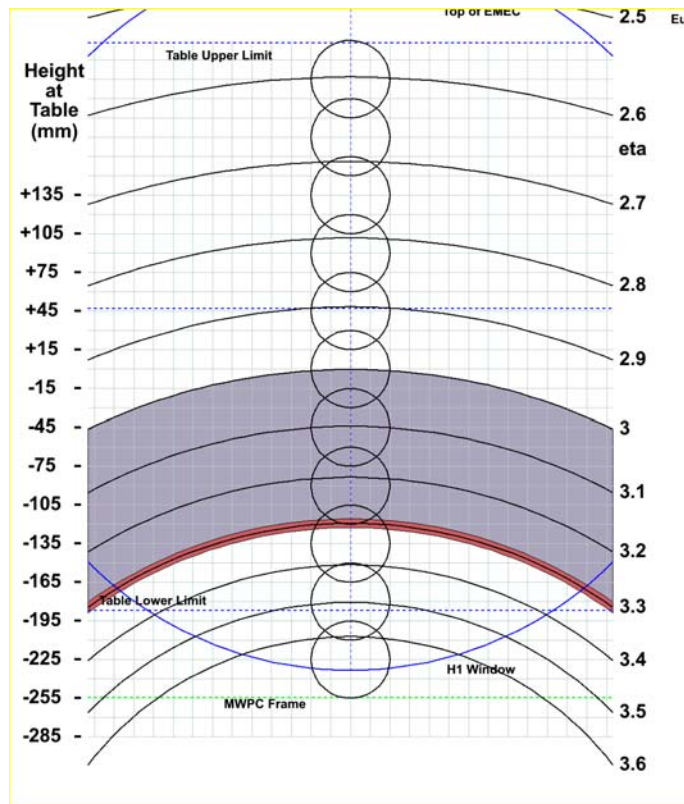


Figure 14. Projected plane at the front face of FCal2 with cryostat raised by 50 mm.

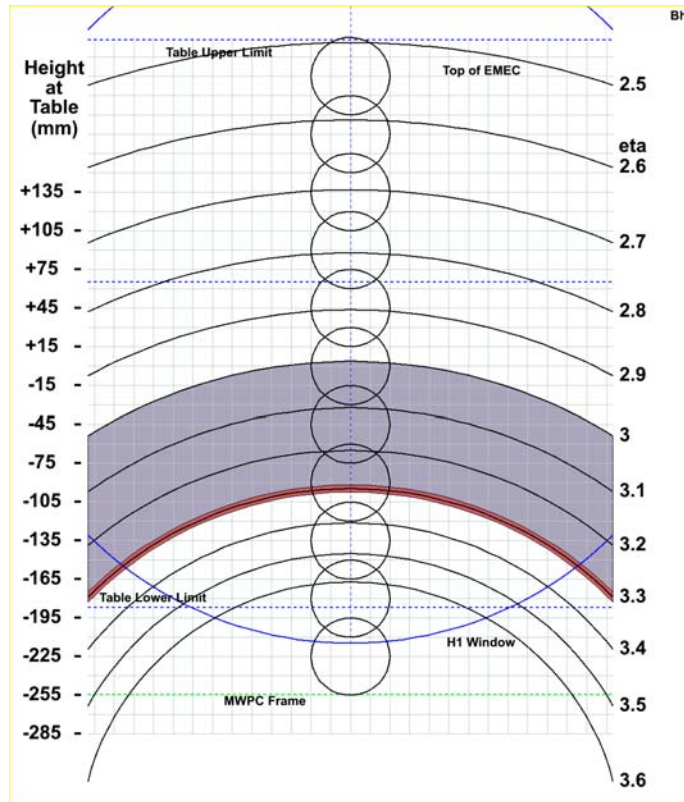


Figure 15. Projected plane at the downstream end of the EMEC with cryostat raised by 70 mm.

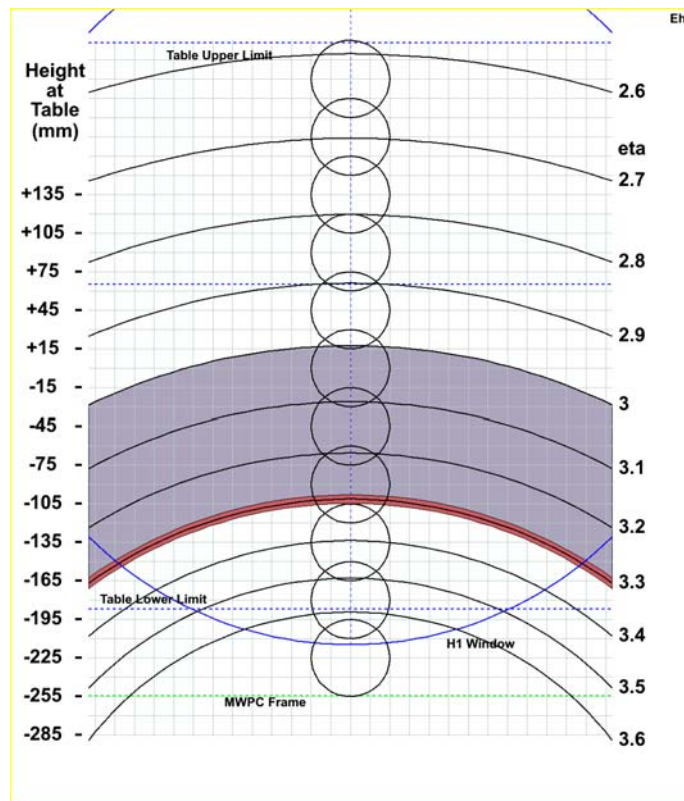


Figure 16. Projected plane at the front face of FCal2 with cryostat raised by 70 mm.

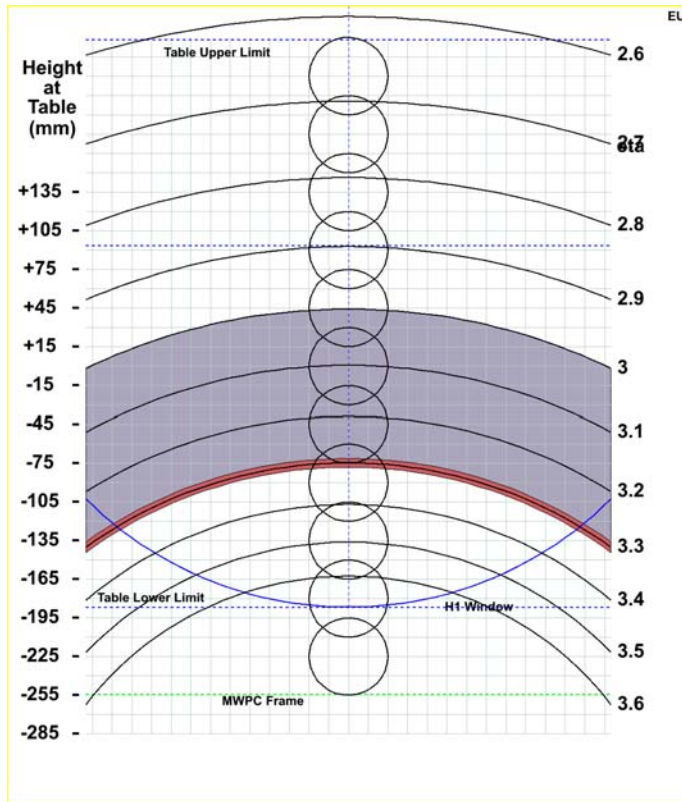


Figure 17. Projected plane at the front face of FCal2 with cryostat raised by 100 mm.

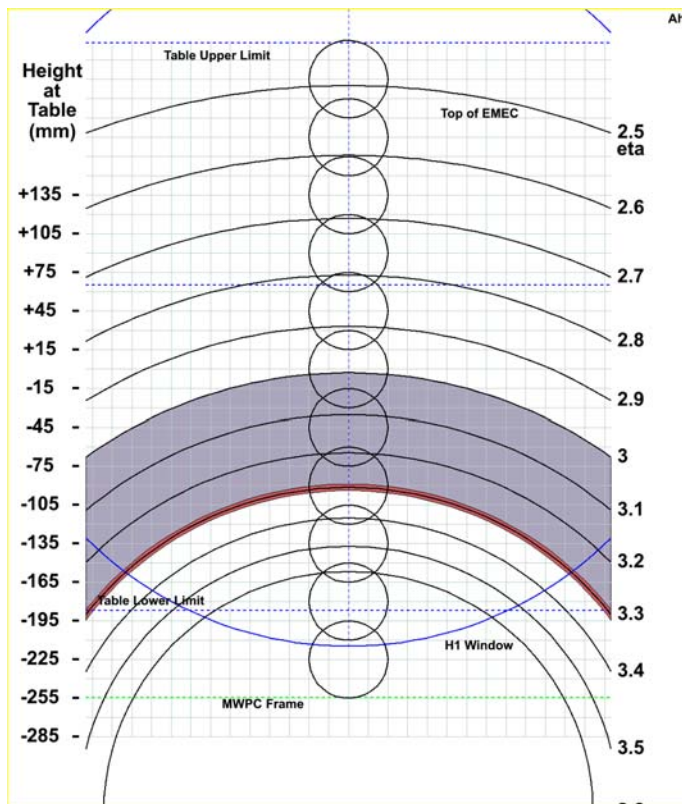


Figure 18. Projected plane at the front face of the EMEC with cryostat raised by 70 mm.

Each projection to the view plane shown in Fig. 11 to 18 is as though recorded by a fixed camera. So the scale of heights on the left is the same in every picture; so also is the light-blue grid, the table upper and lower limits, and the MWPC frame. The heights are with respect to the nominal H6 beam (undiverted by TRIM5 and/or Bend 9). The small circles indicate the “wide” beam spot of 60 mm diameter. The succession of these spots are meant to suggest a possible crack scan strategy with the new, improved Bend 9 at 200 GeV/c. The range covered by the present Bend 9 includes only the middle 7 of 11 “wide” beam spots. Relative to Fig. 11 and 12, the H1 window (and the horizontal dotted line meant to denote the vertical center of the window) is raised in Fig. 13 and 14 by 50 mm, in Fig. 15, 16, and 18 by 70 mm, and in Fig. 17 by 100 mm. In these projected views these heights are slightly smaller as might be noticed by the astute observer. Lines of fixed η and the transitions are shown in each of Fig. 11 to 18. Remember that the EMEC inner wheel covers from $\eta = 2.5$ to $\eta = 3.2$ as seen in both planes A and B. In case a feature does not lie in the plane depicted (e.g. the cone does not extend beyond plane D) then that feature is first projected to the depicted plane along a line of constant η before projection to the view plane at the downstream BPCs.

Plane B is well suited to examining the allowed coverage for electrons in the EMEC inner wheel. And it is not well suited to examining the coverage of particles in the FCal because the FCal is well downstream of this B-plane. Plane E is well suited to examining the coverage of hadrons in the FCal because the upstream face of FCal2 is approximately at hadronic shower maximum for hadrons impinging on the face of FCal1. Plane E can be used for interpolating between Plane B and Plane E for hadronic showers in the HEC.

Fig. 11 shows that it is possible to direct 120 GeV/c (but not 200 GeV/c with the present Bend 9) electrons into the HEC above the EMEC inner wheel (which ends at $\eta = 2.5$ but with structural material for a few cm beyond). Otherwise almost the full region of the EMEC inner wheel (and the HEC behind it) can be scanned with the 200 GeV beam. Fig. 11 also shows that a small portion of the “wide” 200 GeV/c beam at the lower extreme of the present Bend 9 (two circles above the lowest) passes below the cone (consistent with Fig. 7. This does not show up in Fig. 12 because plane E is well downstream of the cone.

In Fig. 12 we can see that with the present Bend 9 we cannot get 200 GeV/c beam into the FCal (with the exception of a small portion of the “wide” beam) and certainly not far enough from the transitions to fully contain an hadronic shower. With an enhanced Bend 9 the next limit to getting beam into the FCal is the table limit. The table goes down as far as -187 mm. Some of the tracking devices on the table can be lowered, effectively increasing the lower limit to about -215 mm (and another 30 mm with “wide” beam to -245 mm). About here we are approaching the frames of the immovable MWPCs on the table and running out of bending power, even with the new Bend 9. This seems too tight to reliably scan the crack region. We are uncomfortably close to several limits, none of which we know with certainty.

If we raise the H1 cryostat by 50 mm, the situation changes. Fig. 13 shows that all the target points (see lettered points in Fig. 8) can still be a part of the program up to 200 GeV/c even with the present Bend 9. However sending 120 GeV electrons above the EMEC inner wheel directly into the HEC now seems problematic. But we can direct 200 GeV/c beam to the top of the EMEC with the new Bend 9. More importantly, Fig. 14 shows we can now direct 200 GeV/c beam into the FCal sufficiently far from the transitions so that showers are as fully contained as possible. This marks the high η extreme of the scan range and is acceptable. So raising the cryostat by 50 mm seems to accomplish our goals in a reasonably optimal way.

Fig. 15 and 16 show the same things but after raising the H1 cryostat by 70 mm instead of 50 mm. Again the same conclusions apply except now the very top of the EMEC is accessible at 200 GeV/c only with “wide” beam. But all the target points are still accessible with “narrow” beam. So the full coverage of the EMEC/HEC gets a bit tighter at the lowest values of η while the comfort margin improves at the highest values of η .

Fig. 17 indicates that raising the cryostat by 100 mm doesn't provide much improvement for the FCal side of the scan (assuming an even slightly enhanced Bend 9) and further limits the reach to the top of the EMEC. So raising the cryostat by 100 mm is not favored.

The proposal, then, is to 1) enhance the bending power of Bend 9 by adding an identical magnet just upstream of the present Bend 9, 2) increase the diameter of the H6 beam line vacuum pipe in the region of Bend 9 so that the flanges which are presently about 120 mm diameter are not a limit, and 3) raise the H1 cryostat by at least 50 mm and preferably by 70 mm to allow a margin for errors in our present understanding of the geometry. These improvements should be completed before the start of the second CBT-EC2 beam period on 11 August so as to make optimal use of our allocated run time and to better insure against loss of beam due to various possible failures.

Because the weight of the liquid argon in the H1 cryostat is more than 10 tonnes and because of safety concerns, we plan to transfer the liquid into the holding dewar, keeping the H1 cryostat cold, while the engineers raise the cryostat. The liquid will then be transferred back when the raising operation is completed. A cryogenics expert will have to be scheduled for this operation because Anatoli Pleskatch is not due to return to CERN until the end of the run period.

A short description of the procedure for raising the H1 cryostat was prepared and then reviewed by Peter Schilly who gave a tentative approval. He requested to be informed about the schedule in case he is at CERN so he can watch. This was not a condition on his approval however. TIS will also look into this matter.

Drawings of the spacer plates which will hold the H1 cryostat at its new height have been prepared and will be sent to the shop shortly. The same is true for the new platform for the H1 cryostat pusher mechanism which moves the cryostat transverse to the beam.

Engineers Leif Shaver from Arizona and Mircea Cadabeschi from Toronto are preparing to come to CERN for this cryostat raising operation. At nearly the same time the FCalC assembly is scheduled to be inserted into the EndCap C Cryostat so the engineers hope to do both operations during the same trip. Final scheduling awaits better information on the FCalC insertion schedule. Martin Aleksa is helping with coordination. It is also possible that Roy Langstaff will be involved.

Run Plan:

A possible run plan is as follows:

Start with 200 GeV/c negative pions (if H8 allows)

Use “wide” beam (60 mm diameter on the BPCs)

Start with the beam spot as high in the EMEC/HEC as desired.

Take 50k events and then step down by 45 mm.

Continue stepping down with 50k events at each step until the cryostat window edge is reached

Repeat this scan at

Lower momenta, down as far as beam rate will allow

With electrons (but only 40k max events)

When finished repeat the negative pion scan again to improve statistics and check on stability of the results

At each momentum set up the CEDAR to detect pions and not protons

References:

[1] ATLAS Liquid Argon Calorimeter Technical Design Report, CERN/LHCC/96-41, ATLAS TDR 2, 15 December 1996.

[2] A.Kiryunin, "Monte Carlo Studies for Combined Test of EMEC, HEC, and FCal (Region $\eta \sim 3.2$)", Transparencies from ATLAS LArG HEC/FCal/Combined test-beam Meeting on 24 April 2001.

[3] ATLAS Detector and Physics Performance Technical Design Report, CERN/LHCC/99-14, ATLAS TDR 14, 25 May 1999.

[4] Sven Menke, MPI Munich, private communication.

[5] Ilias Efthymiopoulos, CERN, private communication.